TEXAS Geosciences
The University of Texas at Austin
Jackson School of Geosciences

Baylor University | Department of Geosciences

EGU General Assembly #vEGU21

Sharing is encouraged

Volcanic forces inferred from EBSD and µXRD analyses of Yellowstone quartz

Omero F. Orlandini[1], Kenneth Befus[2]

[1]Department of Geological Sciences, University of Texas at Austin; [2]Department of Geosciences, Baylor University

Introduction: a record of magmatic processes at the lattice scale

The magnitude of forces at play in active magmatic systems is poorly constrained because direct observation is difficult. Additional complications include short time scales and the likelihood of overprinting signatures of deeper processes by the catastrophic nature of eruption. Deformation of crystal lattices is one signature of magmatic force common to all crystals that survive eruption. Quartz crystals have documented residual elastic stresses in the hundreds of MPa measured using synchrotron µXRD. These stresses may be caused by several processes: crystal-crystal impingement in a crystal mush, explosive fragmentation, or shear in flowing lavas. To better unravel when these stresses were imparted relative to the ultimate eruption, we combine µXRD with new electron back-scatter diffraction (EBSD) measurements. EBSD helps constrain subgrain and twin boundary relationships, geometrically-necessary dislocation density (GND), and plastic deformation.

We target quartz grains from a violent Yellowstone super-eruption and from a large-volume rhyolitic obsidian lava flow (Huckleberry Ridge Tuff and Summit Lake lava, respectively). Samples from both Yellowstone eruptions preserve roughly the indistinguishable amounts of elastic residual stresses, ranging from 100 to 150 MPa. EBSD indicates a GND density of ca. 4E12, with slightly higher values in the Summit Lake Lava. Diffraction peak broadening provides a record of plastic deformation using µXRD. Diffraction peaks are significantly more smeared in Summit Lake lava (0 to 0.15 degrees) than in Huckleberry Ridge Tuff (~0.06 degrees). Subgrain and dauphiné twin formation in both samples is documented by both µXRD and EBSD.

Y45: Huckleberry Ridge

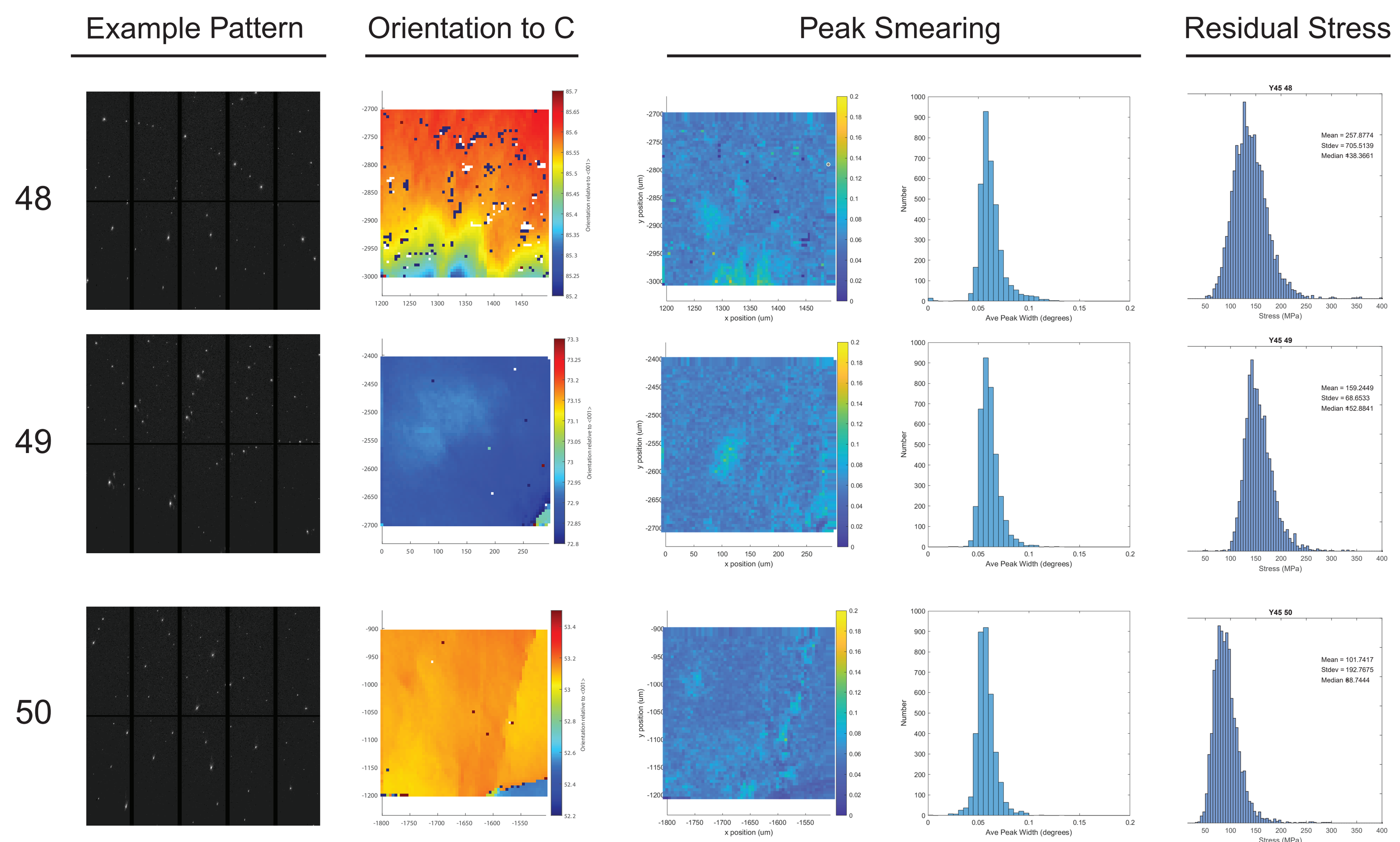

µXRD data (Befus et al., 2019)

Using synchrotron Laue X-ray microdiffraction (µXRD), the elastic strain of quartz crystals can be measured directly by streatching/smearing/misplacing of diffraction patterns. This elastic strain is primarily the result of applied deviatoric stresses on the crystal, and may be preserved as defects or dislocations within the grain's lattice. The reported residual stress for each sample represents the mean and 1σ standard deviation of the individual spot measurements, n, whose distributions produce the stress maps. Residual stress uncertainty is estimated to be ~30 MPa, which we calculated using the observed distribution of residual stress in the undeformed quartz.

Y74: Summit Lake Lava

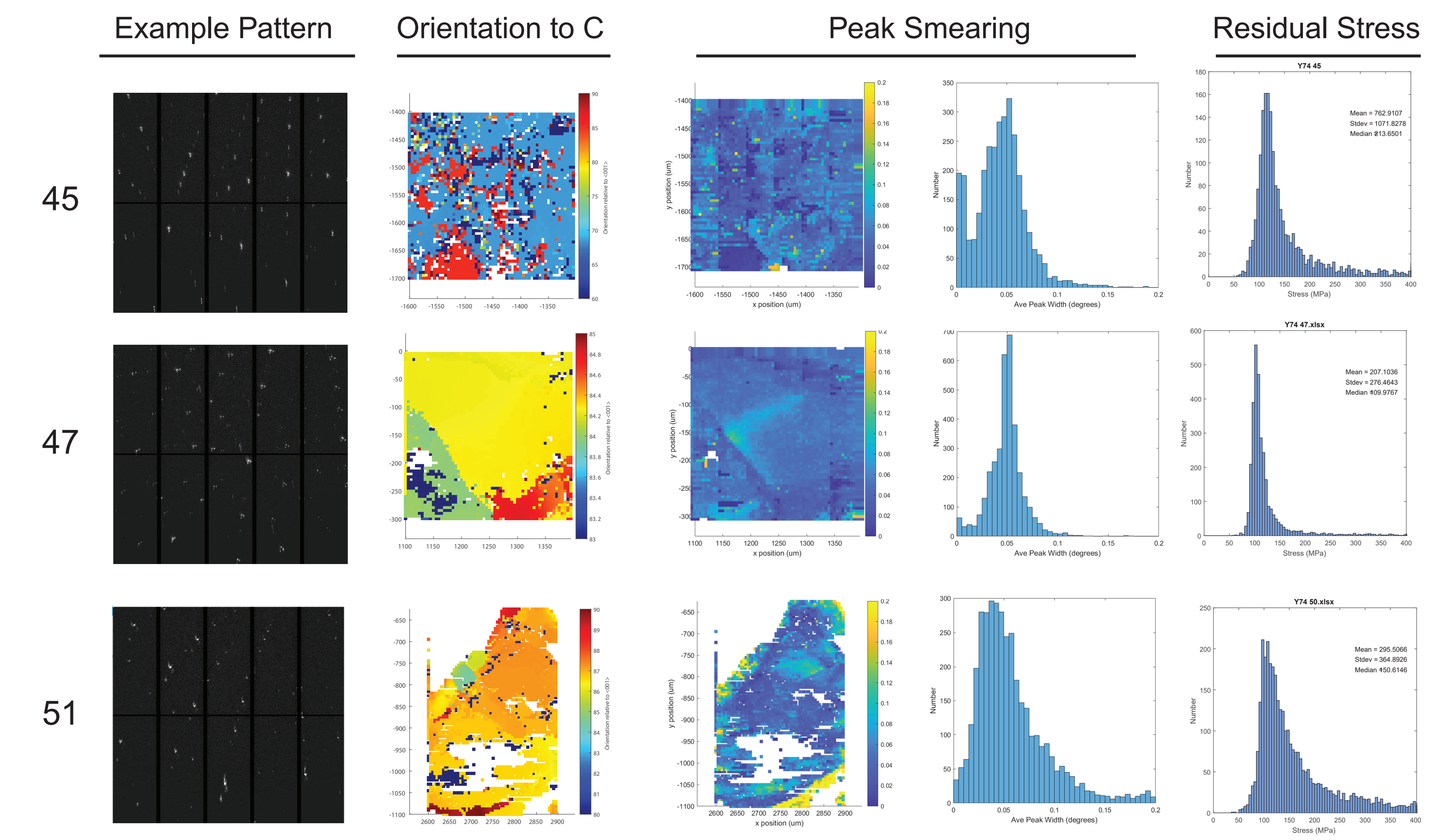

EBSD measurements and derived dislocation density

Because EBSD measures the orientation of a crystal lattice, the curvature of a continous lattice may be measured to an angular precision of 0.03 degrees using the de-noising proposed by Hielscher et al., 2020. By assuming that the curvature is due to the presence of dislocations, the material's known slip systems can be populated with theoretical dislocations until the observed curvature is explained - hence the term 'geometrically-necessary dislocations' (GNDs).

An important distinction between µXRD and EBSD is that each µXRD point is an independent measurement, while EBSD relies on relative misorientations between points.

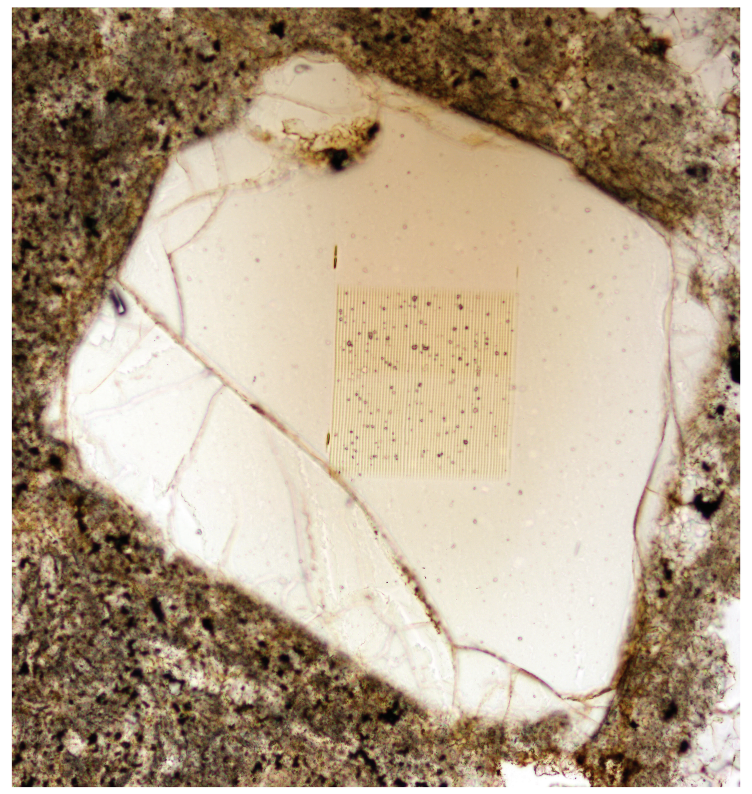

Polarized light micrograph of Huckleberry Ridge sample 45, grain 49, showing µXRD damage to epoxy underlying grain.

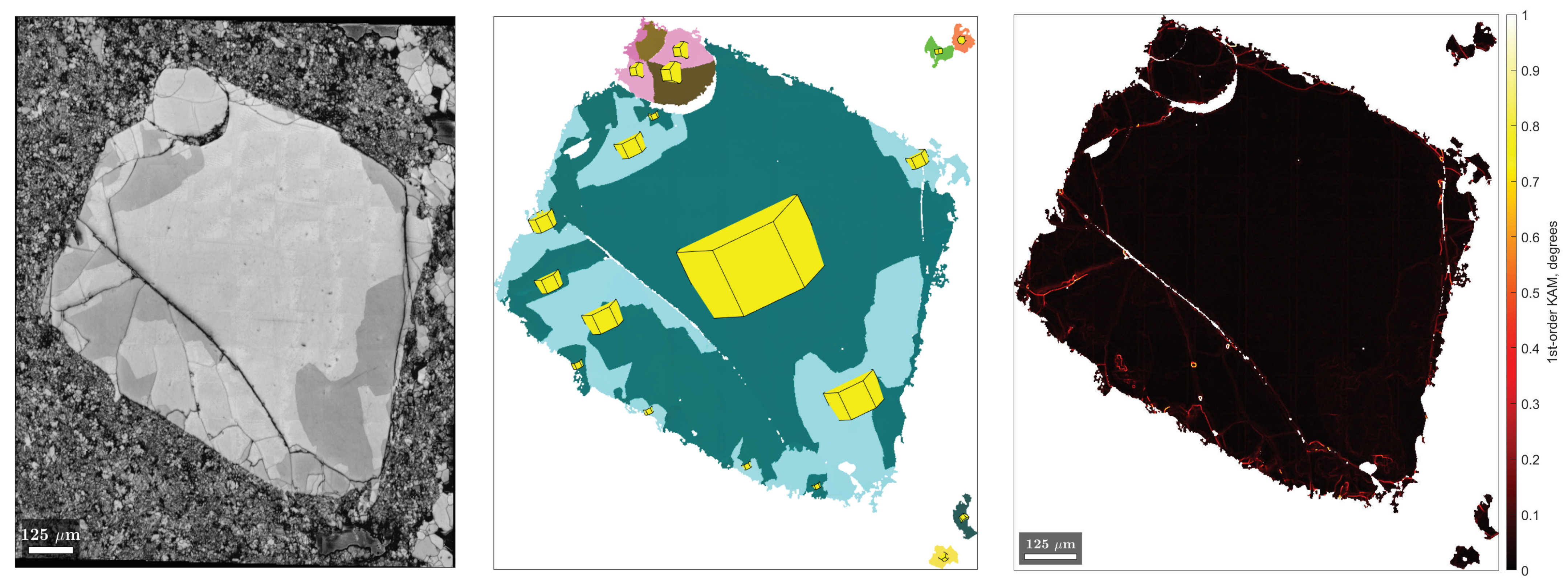

EBSD data from same grain, with band contrast values (left) highlighting dauphiné twins and grain boundaries (light blue vs dark blue, and brown/pink vs blues in center map). Rightmost map shows kernel-averaged misorientation (KAM) with color scale set to 1 degree, illustrating the formation of local dislocation substructures near rim of grain.

Dislocation density piezometry theory and parameters

$$\frac{\sigma}{2\mu} = \alpha(\rho b^2)^{1/k}$$

Twiss 1977's summary of a generic dislocation density piezometer. Dislocations are produced in a crystalline material by the application of differential stress, and their density scales with that stress. A critical point to note is that EBSD can *only* measure GNDs, but another class of dislocations exists which does not contribute to lattice curvature but are still induced by stresses: 'statistically stored dislocations' (SSDs). The proportion of SSD to GND must be inferred or known *a priori*.

ρ	Total dislocation density
α	Material constant of order 1, 1.314 from McCormick, 1977
μ	Shear modulus, 31GPa
b	Burger's vector, 4.9138E-10 m
k	Stress exponent, 2
σ	Differential stress

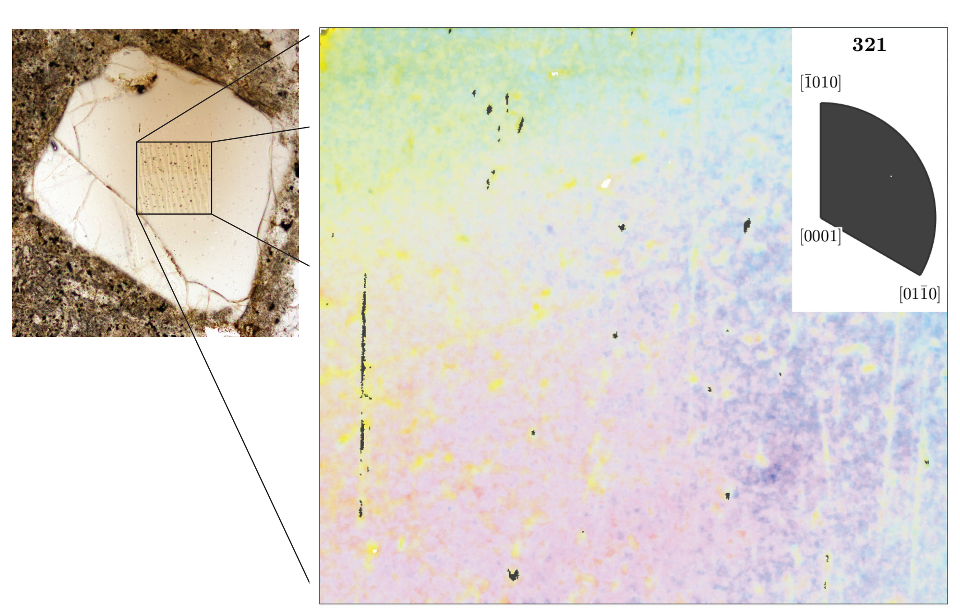

Inverse pole figure map with full color range set to 1 degree from map mean orientation (key on right), illustrating minimal lattice misorientation across map area.

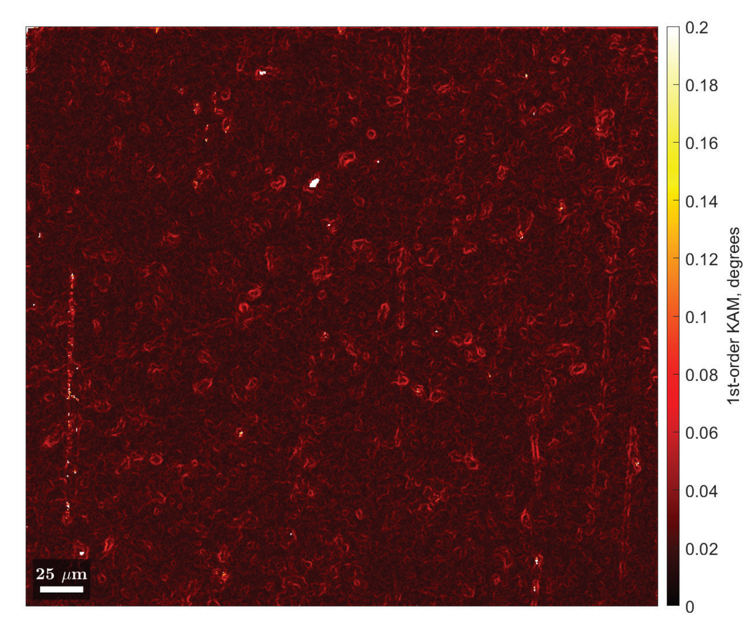

Kernel-averaged misorientation (KAM) map of same area, maximum value set to 0.2 degrees. Linear gouges are from polish.

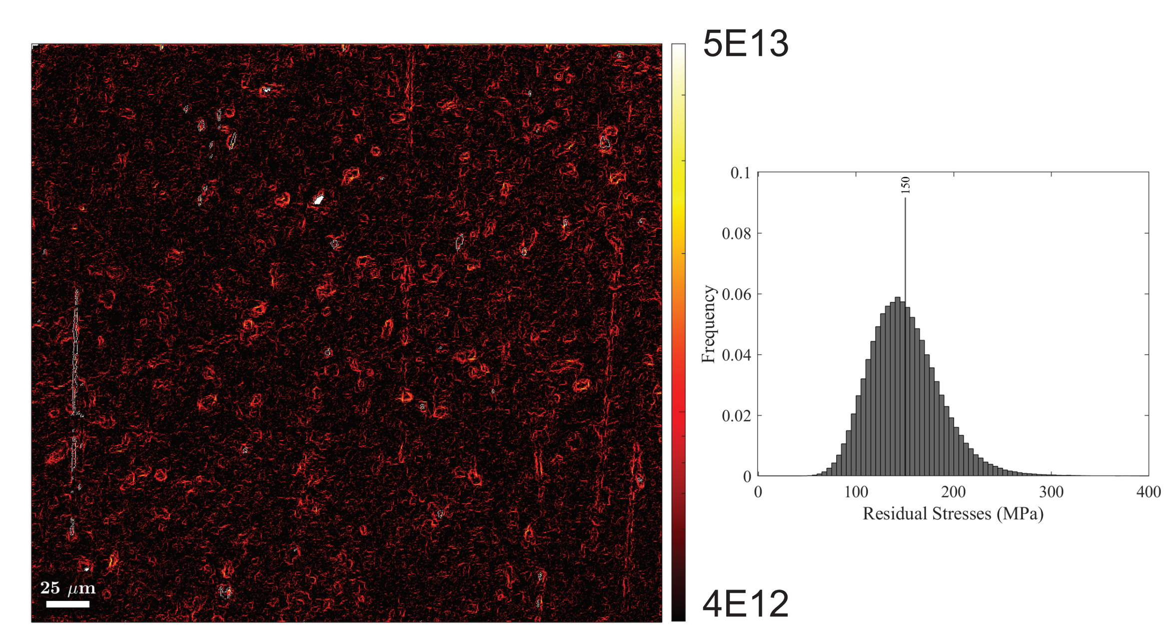

GND density map showing that GND density increases by up to an order of magnitude over ~1 µm distances in abundant local microstructures - an increase of >100 MPa.

Results and discussion

Sample	Grain	step size (µm)	Mean GND density	EBSD stresses (MPa) Mean	EBSD stresses (MPa) 2σ	EBSD stresses (MPa) GND %	µXRD Stresses (MPa) Mean	µXRD Stresses (MPa) 2σ
Y45b	48	0.5	4.19E+12	264	110	7.1	257	705
	49	0.3	3.85E+12	150	73	20.0	159	68
		0.5	3.11E+12	161	65	14.3		
	50	0.5	2.23E+12	111	77	20.0	101	192
Y74	45	0.5	4.52E+12	759	409	0.9	762	1071
		0.5	4.84E+12	775	362	1.0		
	47	0.5	4.03E+12	203	124	11.1	207	276
		0.5	3.65E+12	209	84	10.0		
		0.5	3.86E+12	203	89	11.1		
	51	0.5	3.65E+12	293	137	5.0	295	364
		0.5	3.58E+12	294	212	4.5		
		0.5	3.47E+12	296	110	4.8		

As shown in Befus et al. 2019, µXRD shows little difference in the residual stresses in quartz grains from of the two Yellowstone eruptions, despite their dramatic difference in eruptive styles. EBSD-derived dislocation densities suggest stresses in agreement with published µXRD values from the same grains.

We conclude that elastic residual stresses record pre-eruptive magmatic environment. Viscous shear during lava emplacement generates the majority of plastic deformation, which swamps the signal of lesser amounts of plastic deformation produced in the reservoir or conduit. Pre-eruption processes are likely the source of elevated elastic residual stresses, and we favor an interpretation where the stresses arise from force-chain impingements within crystal mushes prior to eruption.

This study also illustrates the complementary nature of µXRD with EBSD. EBSD quickly and inexpensively shows microstructure within potential or former µXRD targets at the cm to the nm scale. Many of the microstructures illustrated in this study by EBSD, such as the ellipsoidal features in the maps to the left, are masked by the coarser spatial resolution of µXRD and require further investigation. Further, reasonably accurate calculation of GND densities by EBSD is a recent innovation and much is yet to be learned. In particular, proportions of GND to SSD are not well studied, and the significantly lower GND fraction inferred for the Summit Lake lavas may be the result of prolonged cooling and thus recovery of the more-mobile GNDs, or it could be due to the grain-scale strain heterogeneities observed in EBSD.

Befus, K.S., Manga, M., Stan, C., Tamura, N., 2019. Volcanoes Erupt Stressed Quartz Crystals. Geophysical Research Letters 46, 8791–8800. https://doi.org/10.1029/2019GL083619

Hielscher, R., Silbermann, C.B., Schmidla, E., Ihlemannb, J., 2019. Denoising of crystal orientation maps. Journal of Applied Crystallography 52, 984–996. https://doi.org/10.1107/S1600576719009075

Twiss, R.J., 1977. Theory and applicability of a recrystallized grain size paleopiezometer. Pure and Applied Geophysics PAGEOPH 115, 227–244. https://doi.org/10.1007/BF01637105